

MICROWAVE INTERFEROMETRY FOR PLASMA STUDIES*

By L. C. ROBINSON† and L. E. SHARP†

A beam of microwave radiation is a powerful and penetrating means of exploring the density and temperature of laboratory plasmas while causing minimal perturbation of the plasma. To a wave of frequency greater than the electron plasma frequency the plasma behaves like a dielectric, causing a change in the "optical" path which, when measured by interference techniques, yields the average electron density. The attenuation of the probing wave can give the collision frequency and hence the plasma temperature.

Propagation Equations

Representing a plane wave by the notation $e^{j\omega t - \gamma r}$ we can determine the propagation constant γ from the well-known Appleton-Hartree dispersion relation. If we restrict consideration to the case of propagation transverse to the confining magnetic induction field with the E -vector of the wave parallel to this field, the dispersion relation is given by

$$\gamma = \alpha + j\beta = j\frac{\omega}{c} \left(1 - \frac{\omega_p^2}{\omega} \cdot \frac{\omega + j\nu}{\omega^2 + \nu^2} \right)^{\frac{1}{2}}, \quad (1)$$

where ν is the collision frequency. For the plasma used in these experiments ν is much less than the wave frequency ω and the plasma frequency $\omega_p = (n_e e^2 / \epsilon_0 m_e)^{\frac{1}{2}}$.

In the three frequency regions of interest, $\omega > \omega_p$, $\omega = \omega_p$, and $\omega < \omega_p$, the attenuation constant α and the phase constant β are found from equation (1):

$$\omega > \omega_p \gg \nu, \quad \alpha = (\omega_p^2 \nu / 2c\omega^2)(1 - \omega_p^2/\omega^2)^{-\frac{1}{2}}, \quad (2)$$

$$\beta = (\omega/c)(1 - \omega_p^2/\omega^2)^{\frac{1}{2}}, \quad (3)$$

$$\omega = \omega_p \gg \nu, \quad \alpha = \beta = (1/c)(\frac{1}{2}\omega_p \nu)^{\frac{1}{2}}, \quad (4)$$

$$\omega_p > \omega \gg \nu, \quad \alpha = (\omega/c)(\omega_p^2/\omega^2 - 1)^{\frac{1}{2}}, \quad (5)$$

$$\beta = (\omega_p^2 \nu / 2c\omega^2)(\omega_p^2/\omega^2 - 1)^{-\frac{1}{2}}. \quad (6)$$

Equation (3) gives the electron density in terms of the measured phase shift and (2) gives the collision frequency from the measured attenuation and known density. Provided the electron-ion collision frequency is somewhat larger than the electron-neutral gas collision frequency the electron temperature (T_e , in degrees Kelvin) can be calculated from the expression (Delcroix 1960)

$$\nu = (2 \cdot 6n \ln A) / T_e^{3/2}, \quad \text{collisions/s}, \quad (7)$$

* Manuscript received May 15, 1963.

† Wills Plasma Physics Department, School of Physics, University of Sydney.

where $\ln A$ is an insensitive function of temperature, n is the number density of the plasma in electrons/cm³, and T_e is the temperature in degrees Kelvin.

When the plasma frequency rises to and beyond the probing frequency the attenuation (given by (4) and (5)) becomes very large and transmission is "cut off".

Interferometers

The plasmas used in these interferometry studies were produced in the cylindrical metal vessels of the Supper I (diameter 15 cm) and Supper II (diameter 21 cm) machines at Sydney University, by the discharge of a pulse-forming network between the cylinder and a short central electrode at one end of the machine (Brennan *et al.* 1963). The resulting plasma was transient in nature and was contained by a strong axial magnetic induction field for some hundreds of microseconds. Its kinetic temperature was known to be about 1 eV, so that during the wave transmission period the electron-ion collision frequency was much less than the microwave frequency (35 kMc/s), as assumed in the equations above.

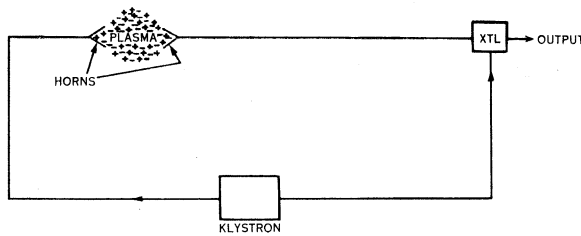


Fig. 1.—Schematic drawing of a simple interferometer.

A microwave probing beam with the E -vector parallel to the magnetic induction field was launched from a waveguide horn placed in the plasma vessel but withdrawn a half-inch outside the outer wall, and received by a similar horn located diametrically opposite.

The simplest, and historically the first, type of interferometer used for phase measurements is that shown diagrammatically in Figure 1. Here the signal from an 8 mm wavelength klystron, after being split into one beam which traverses the plasma and another which negotiates a reference path, is recombined in the crystal mixer. If we assign amplitudes A and B respectively to the reference and probing waves at the mixer crystal (assumed to be operating in the square-law region of its characteristic) it is easily shown that the crystal current is $AB \cos \beta(t)l$, where $\beta(t)l$ is the time-dependent phase shift produced by the transient plasma, $\beta(t)$ being the phase constant of equation (3), l the thickness of the plasma, being taken as the internal diameter of the containing vessel, and B is the product of the amplitude of the unattenuated probing wave and $e^{-\alpha l}$. This waveform, when displayed on a C.R.O., gives interference patterns similar to those of Figure 2. Density information derived from the period of the pattern of Figure 2(a) is given in Figure 3.

It should be noted from these interference patterns that signals are still transmitted during cut-off despite the large attenuation predicted by (4) and (5). This effect is believed to be due to propagation in the annular "waveguide" formed by the vessel wall and the outer surface of the cut-off plasma—a contention supported by the reflection observations.

This simple interferometer has a serious disadvantage: unless the density approaches "cut-off" so that the amplitude varies, it is impossible to decide whether the density is rising or falling; beyond this the instrument has advantages that will be elaborated later.

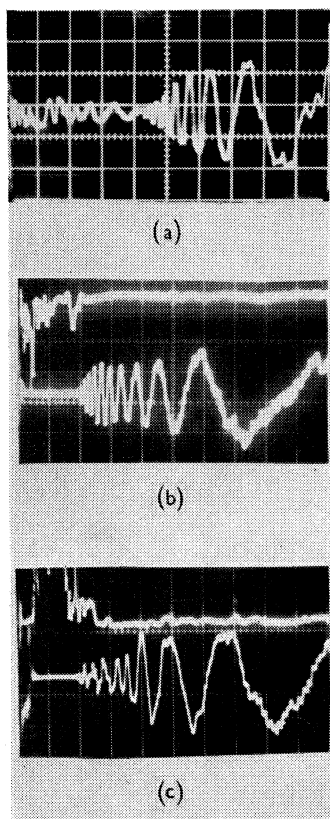


Fig. 2.—Simple interferometer patterns: (a) For a hydrogen plasma in Supper I at 55 microns initial neutral pressure. The axial magnetic field is 5 kG. The sweep rate is $100 \mu\text{s}/\text{cm}$ and the true interference pattern starts after $420 \mu\text{s}$. (b) For a hydrogen plasma in Supper II at 1.0 micron initial neutral pressure, with the reflected signal displayed above it. The axial magnetic field is 5.1 kG and the sweep rate is $200 \mu\text{s}/\text{cm}$. (c) For a hydrogen plasma in Supper II at 0.7 micron initial neutral pressure, with the reflected signal displayed below it. The axial magnetic field is 5 kG and the sweep rate is $200 \mu\text{s}/\text{cm}$.

An instrument which yields this information is shown in Figure 4 (see Drummond 1961). The klystron output is frequency modulated and passed through a long length of waveguide whose dispersive characteristic produces two wavelengths phase shift of the probing wave. When this is mixed with a short reference path signal two wavelengths of a sinusoidal waveform result from each sawtooth sweep of the klystron reflector voltage. Pulses produced by clipping and differentiating this waveform are used to intensity modulate a C.R.O. trace which is vertically

displaced by the sawtooth modulation voltage and horizontally swept at a slower rate as shown in Figure 4(b). The resulting pattern of bright spots on the screen

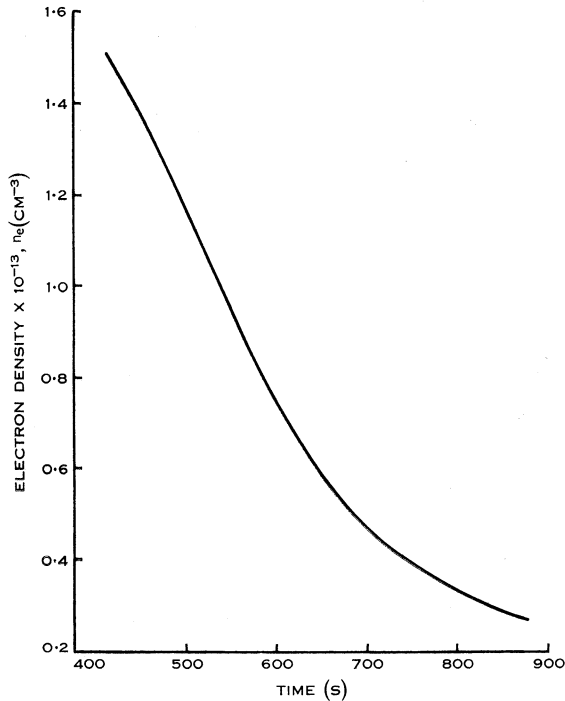


Fig. 3.—Electron density as a function of time derived from the pattern of Figure 2(a).

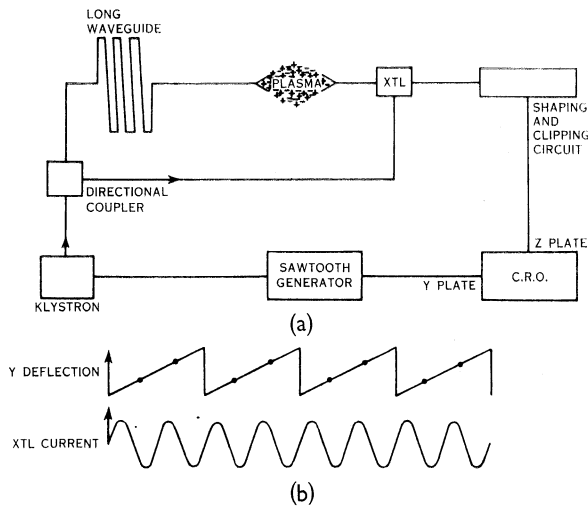


Fig. 4.—Schematic drawing of a band-presentation interferometer.

appears as two bands or fringes. A varying plasma density changes the period of the interference waveform and hence is displayed as vertical displacements of the bands.

In Figure 5 interference patterns produced by this instrument are shown. The steep descending lines indicate a decaying plasma while the appearance of each new band signifies a phase decrease through the plasma of 2π radians.

This interferometer, then, displays density in a convenient manner and shows whether it is rising or falling. However, this information is obtained at the expense of a substantial sacrifice of response time. Temperature can be obtained from the amplitude of the waveform prior to clipping. If we specify that a minimum of

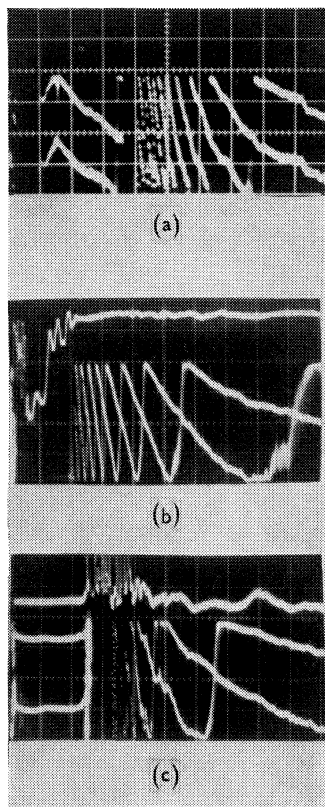


Fig. 5.—Band-presentation interferometer patterns: (a) For a hydrogen plasma in Supper I at 55 microns initial neutral pressure. The axial magnetic field is 5 kG. This display should be compared with that of Figure 2(a), which was obtained for an identically prepared plasma. (b) For a hydrogen plasma in Supper II at 1.0 micron initial neutral pressure with the reflected signal displayed above it. The axial magnetic field is 5.1 kG and the sweep rate is 200 $\mu\text{s}/\text{cm}$. This display should be compared with that of Figure 2(b), which was obtained for an identically prepared plasma. (c) Interference pattern for a hydrogen plasma in Supper II at 0.7 micron initial neutral pressure with the reflected signal displayed above it. The axial magnetic field is 5 kG and the sweep rate is 200 $\mu\text{s}/\text{cm}$. This display should be compared with that of Figure 2(c), which was obtained for a similarly prepared plasma. Note the 250 μs delay in the breakdown of the gas, after the application of the radial electric field.

10 spots are required to satisfactorily display a fringe shift, it follows that a fringe shift must not take place in less than 10 periods of the sawtooth, or 20 μs when we use a modulation as high as 500 kc/s. This limitation is apparent from the dotted nature of the bands in Figure 5.

We note, in Figure 5(a), the appearance of “ghost” bands due to propagation around the cut-off plasma. Because of the confusion caused by this effect the transition from cut-off to cut-on must often be determined by observations of microwave reflections from the plasma, as shown in the upper traces of Figures 2(b) and 5(b), above the interference patterns. In general, reflection signals give a definite indication of cut-on; however, in some cases their accuracy is limited. We have experienced

this particularly with plasmas just above cut-off (see Figs. 2(c) and 5(c)), presumably because only a small region of the plasma has risen above cut-off, thereby producing only small reflections, while scattering around this region is significant. Nevertheless, reflection measurements are always useful and often essential to the interpretation of interference patterns.

By observing reflected signals we have obtained valuable information about the movements of the plasma boundary. The periodic nature of the reflected signals results from interference between a wave of constant phase reflected from the cut-off boundary of the plasma. One period of this pattern indicates the time taken by the plasma boundary to move through one half-wavelength, thereby giving the boundary velocity.

TABLE I
COMPARISON OF INTERFEROMETER CHARACTERISTICS

Characteristic	Simple Interferometer	Band-presentation Interferometer
Information given	N_e T_e Containment time Thickness of plasma (if cut-off is reached) dN_e/dt and its sign only if cut-off is approached and the collision frequency not too small	N_e T_e (indirectly) Containment time Thickness of plasma (if cut-off is reached) dN_e/dt and its sign
Convenience of display	Fair	Good
Transient response	Good	$>20 \mu s$

In Table I the merits and disadvantages of each type of interferometer are set out for comparison.

The band-presentation interferometer is particularly useful when the phase shift is linearly related to density, in which case the display is a direct measure of density. From the expansion of equation (3) we find that this linear condition is satisfied provided the plasma density does not exceed about 40% of the cut-off density. On the other hand, the simple interferometer has the advantage of rapid response performance while being considerably less expensive and much less wasteful of klystron power. The importance of this latter point is apparent when we realize that the waveguide required to produce two wavelengths of dispersion introduces at least 8 dB loss in the present 8-mm instrument. For studies of higher densities where 1 and 2-mm sources are necessary, waveguide losses are so great that this instrument is severely handicapped.

Standing-wave Interferometer

The interferometer shown in Figure 6 is here proposed as an instrument which has the simplicity and advantages of the simple interferometer described above but which, in addition, decides whether the density is rising or falling. It will be seen

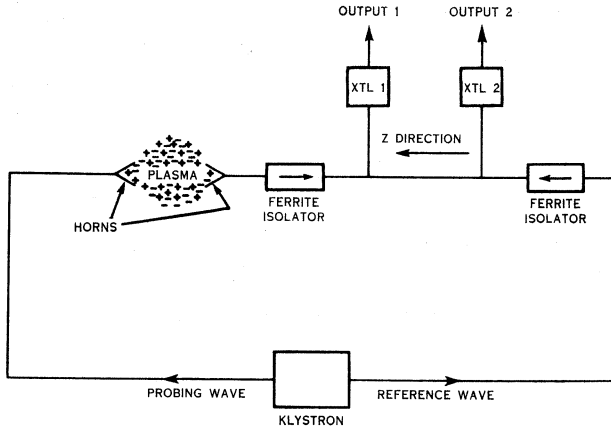


Fig. 6.—Schematic drawing of a standing-wave interferometer.

that the travelling waves from the signal and reference paths are propagated through a waveguide in opposite directions, thereby producing a standing-wave interference pattern which is sampled by two standing-wave detector probe units, and thereafter displayed on a double-beam oscilloscope.

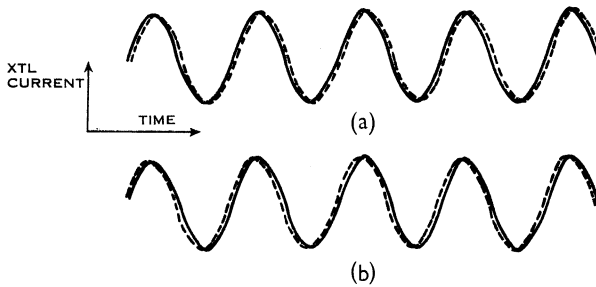


Fig. 7.—Diagram of the predicted output signals from the standing-wave interferometer. Dashed lines represent current in XTLL; full lines, current in XTLL.

If we represent the reference travelling wave by $Ae^{i(\omega t - \beta z)}$ and the probing wave by $Be^{i(\omega t + \beta z + \beta(t)l)}$ (where again the $e^{-\alpha l}$ term is absorbed in B) it is easy to show that the outputs of the square-law crystal detectors 1 and 2 are proportional to $AB \cos(2\beta z_1 - \beta(t)l)$, and $AB \cos(2\beta z_2 - \beta(t)l)$, where z_1 and z_2 are the positions of probes 1 and 2 respectively from some arbitrary fixed plane. From either of these equations we note that the position of the standing-wave pattern moves in the direction of increasing z as the phase of the probing wave increases during plasma

decay, and, conversely, it moves in the negative z direction when the density is rising. The direction of movement, then, of the standing wave pattern tells us whether the density is rising or falling. This movement can be determined as follows. Suppose we locate probe 1 a distance (say) $\frac{1}{8}\lambda_g$ or $\frac{1}{2}n\lambda_g + \frac{1}{8}\lambda_g$, where $n = 0, 1, 2 \dots$, in the positive z direction from probe 2 and observe both crystal outputs on a double-beam oscilloscope. If the pattern observed is similar to that shown in Figure 7(a), that is, probe 2 displays the pattern slightly ahead of probe 1, it is clear that the pattern movement must be in the $+z$ direction and hence the plasma density must be falling. Should the patterns be displaced as in Figure 7(b) the density must be rising.

This standing-wave interferometer, then, decides whether the density is increasing or decreasing, while at the same time retaining all the advantages of the earlier simple instrument listed in Table I. Experimental studies of this interferometer are presently under way, the results of which will be published at a later date.

The authors wish to thank Professor H. Messel, the several Australian manufacturers, and the Australian Institute of Nuclear Science for providing the research facilities which made this work possible.

References

- BRENNAN, M. H., *et al.* (1963).—*Aust. J. Phys.* **16**: 340.
DELCROIX, J. L. (1960).—“Introduction to the Theory of Ionized Gases.” (Interscience Publishers: New York.)
DRUMMOND, J. E. (1961).—“Plasma Physics.” (McGraw-Hill: New York.)